Proc. Natl. Acad. Sci. USA
Vol. 91, pp. 11467–11471, November 1994
Biochemistry

NMR analysis of tRNA acceptor stem microhelices: Discriminator base change affects tRNA conformation at the 3′ end

(initiator tRNA/protein RNA recognition/aminoacyl-tRNA synthetase/methionyl-tRNA transformylase/elongation factor Tu)

ELISABETTA VIANI PUGLISI*†, JOSEPH D. PUGLISI†‡, JAMES R. WILLIAMSON‡, AND UTTAM L. RAJBHANDARY*

Departments of *Biology and ‡Chemistry, Massachusetts Institute of Technology, Cambridge, MA 02139

Communicated by I. Tinoco, Jr., August 8, 1994

ABSTRACT **An important step in initiation of protein synthesis in *Escherichia coli* is the specific formylation of the initiator methionyl-tRNA (Met-tRNA) by Met-tRNA transformylase. The determinants for formylation are clustered mostly in the acceptor stem of the initiator tRNA. Here we use NMR spectroscopy to characterize the conformation of two RNA microhelices, which correspond to the acceptor stem of mutants of *E. coli* initiator tRNA and which differ only at the position corresponding to the "discriminator base" in tRNAs. One of the mutant tRNAs is an extremely poor substrate for Met-tRNA transformylase, whereas the other one is a much better substrate. We show that one microhelix forms a structure in which its 3′-ACCA sequence extends the stacking of the acceptor stem. The other microhelix forms a structure in which its 3′-UCCA sequence folds back such that the 3′-terminal A22 is in close proximity to G1. These results highlight the importance of the discriminator base in determining tRNA conformation at the 3′ end. They also suggest a correlation between tRNA structure at the 3′ end and its recognition by Met-tRNA transformylase.**

Protein synthesis in *Escherichia coli* is initiated with formylmethionyl-tRNA (fMet-tRNA). A crucial step in this process is the specific formylation of methionine attached to $tRNA^{fMet}$ by Met-tRNA transformylase (EC 2.1.2.9) (1, 2). We showed previously that the major determinants for formylation are clustered in the acceptor stem of tRNA (3). One of these determinants is a mismatch (as found in $tRNA^{fMet}$) or a weak base pair at the end of the acceptor stem. tRNAs carrying the wild-type C1×A72 or virtually any other mismatch are good substrates, whereas those carrying stable base pairs such as C1·G72 or G1·C72 are extremely poor substrates (4–6). These results suggest a requirement for nucleotides 1 and 72 to be unpaired during formylation.

The strong negative effect of C1·G72 or G1·C72 base pairs on formylation can be compensated for by an additional mutation of A73, the discriminator base, which precedes the CCA sequence common to all tRNAs, to a pyrimidine such as U73 (4). For example, in contrast to the C1·G72 mutant, which is a very poor substrate (V_{max}/K_m^{app} down by a factor of 495 compared to wild-type tRNA), the C1·G72/U73 mutant is almost as good a substrate as wild-type tRNA (V_{max}/K_m^{app} down only by a factor of 3.7). Similarly, compared to the G1·C72 mutant, the G1·C72/U73 mutant is a better substrate for Met-tRNA transformylase (V_{max}/K_m^{app} down by a factor of 60, while the factor is 1035 for the G1·C72 mutant). On the basis of these results, we proposed that the discriminator base influences the stability of the terminal base pair in the acceptor stem and/or structure of tRNA at the 3′ end (4, 6).

In this paper, we use NMR spectroscopy (7) to study the effect of the discriminator base (8) on tRNA conformation at the 3′ end. Two RNA oligonucleotides that correspond to variants of the acceptor stem of initiator $tRNA^{fMet}$ were designed for NMR study (Fig. 1*A*). These oligonucleotides contain the seven base pairs of the acceptor stem, in which the nucleotides corresponding to C1 and A72 in the tRNA are changed to a G·C base pair and the bottom of the acceptor stem is capped by a stable -UUCG- tetraloop (9). The two variants differ only at the position corresponding to the discriminator base in tRNA. The A19 variant corresponds to a tRNA mutant that is essentially not formylated, and the U19 variant corresponds to a tRNA that is formylated, although at a lower rate than the wild-type tRNA (6). Comparison of the conformations of the two variants demonstrates the crucial role of the discriminator base in influencing tRNA structure. In the A19 variant, the 3′-ACCA sequence extends the helical configuration of the stem. In the U19 variant, the 3′-UCCA sequence folds back toward the 5′ end of the molecule.

MATERIALS AND METHODS

RNA Synthesis and Purification. Two oligoribonucleotides, 5′-pGGCGGGGUUCGCCCCGCCACCA (referred to as the A19 variant) and 5′-pGGCGGGGUUCGCCCCGCCUCCA (U19 variant), were synthesized in milligram quantities *in vitro* by using T7 RNA polymerase (10). The reaction was primed by GMP and the product was purified by electrophoresis on denaturing polyacrylamide gels (11). Homogeneity of the 3′ end was verified in pilot reactions by complete T1 RNase digestion and homochromatography (12) of ^{32}P-labeled RNA product. Homogeneity of the 5′ end was verified by T2 RNase digestion followed by two-dimensional thin-layer chromatography. Purified RNA was precipitated and dialyzed against 50 mM NaCl/10 mM sodium phosphate, pH 6.5/0.1 mM EDTA. All NMR experiments were performed in this buffer. Both variants formed monomolecular structures at millimolar concentrations as demonstrated by gel filtration chromatography using a Bio-Sil SEC 125 column (Bio-Rad).

NMR Spectroscopy. NMR experiments were performed on a Varian VXR-500 or Unity+ 500-MHz spectrometer. To compare the effects of temperature on conformation, some experiments were performed at 10°C, 25°C, 37°C, and 50°C. Exchangeable proton resonances were assigned by using one-dimensional or two-dimensional nuclear Overhauser enhancement (NOE) experiments. H_2O resonance was suppressed by using binomial (13) or shaped-pulse (14) suppression methods. Nonexchangeable proton resonances were assigned by using a combination of NOE spectroscopy (NOESY), double-quantum filtered correlated spectroscopy

The publication costs of this article were defrayed in part by page charge payment. This article must therefore be hereby marked "*advertisement*" in accordance with 18 U.S.C. §1734 solely to indicate this fact.

Abbreviations: NOE, nuclear Overhauser enhancement; NOESY, NOE spectroscopy; DQF-COSY, double-quantum filtered correlated spectroscopy.

†Present address: Department of Chemistry and Biochemistry, University of California, Santa Cruz, CA 95064.

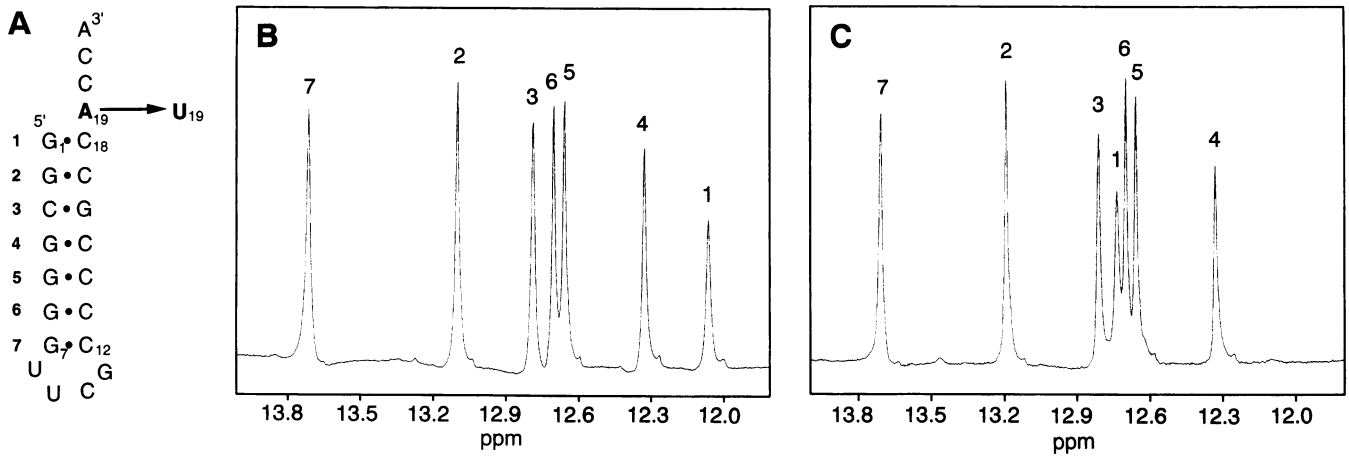

FIG. 1. (*A*) Sequence and secondary structure of the two oligonucleotides corresponding to variants of the acceptor stem of *E. coli* initiator $tRNA^{fMet}$. The 1·18 base pair, corresponding to nucleotides 1 and 72 in the tRNA, is G1·C18 in both variants. The discriminator base 19, corresponding to position 73 in tRNA, is either an adenine (A19 variant) or a uracil (U19 variant). The numbering of the base pairs corresponds to the imino proton resonances in *B* and *C*. (*B* and *C*) Imino proton spectrum of the A19 variant (*B*) and U19 variant (*C*) in 50 mM NaCl/10 mM sodium phosphate/0.1 mM EDTA, pH 6.5 at 25°C.

(DQF-COSY), and total correlated spectroscopy (TOCSY) experiments (15). Structural constraints were obtained from NOESY experiments performed at 50-, 150-, or 400-ms mixing times. Coupling constants for ribose protons were obtained from DQF-COSY experiments.

RESULTS

Design of Oligonucleotides for Study. Our goal was to use NMR analyses to compare the structure of oligonucleotides that differ only at the position corresponding to the discriminator base (8) in tRNAs and that had a clear effect on function of the corresponding tRNA. Transcription by T7 RNA polymerase is currently the method of choice for producing RNAs of the size and amount required. However, this enzyme has a strong preference for initiating RNA chains with a G nucleotide (10). Therefore, the oligonucleotides selected for NMR analyses (Fig. 1*A*) corresponded to the G1·C72 and G1·C72/U73 mutants of *E. coli* initiator tRNA rather than the C1·G2 and the C1·G72/U73 mutants.

Exchangeable Proton Spectra. Imino and most amino protons of the two variants (Fig. 1 *B* and *C*) were assigned by one-dimensional and two-dimensional NOE experiments. The imino proton spectra of both variants show the presence of 7 G·C base pairs as expected for the helical portion of hairpin structure. Resonance number 8 at 10.5 ppm (not included in Fig. 1*B*) corresponds to the imino proton of a G·U base pair as expected in a UUCG tetraloop (9). A sharp imino resonance of the first base pair G1·C18 is present in the spectra of both variants at 15°C (data not shown) and at 25°C (Fig. 1 *B* and *C*). However, the G1·C18 imino proton for the A19 variant resonates at 0.6 ppm upfield from its chemical shift in the U19 variant. These chemical shift differences reflect a difference in local environment due to the presence of A19.

The temperature dependence of the imino proton spectra (data not shown) also reveals differences between the two variants. The G1·C18 imino proton resonance of the U19 variant is considerably broadened at 37°C and is not observed at 50°C. In contrast, the G1·C18 resonance of the A19 variant remains sharp at 37°C and is broadened only at 50°C. The differences between the two variants are restricted to the G1·C18 base pair, since the G2·C17 base pair resonance broadens at a similar temperature for both mutants.

Nonexchangeable Proton Spectra. Spectral assignments for the nonexchangeable proton resonance were made according to methods previously reported (7, 16). All base protons, and ribose H1′, H2′, H3′, and part of H4′, H5′/H5″ were assigned for both molecules.

Structure of the Stem–Loop Region. The 7-bp stem regions of both variants adopt A-form helical conformations as shown by the standard set of internucleotide NOE connectivities observed in this region (Fig. 2 *A* and *B*). The ribose sugars in the helices adopt primarily 3′-*endo* conformations as indicated by the absence of 1′–2′ coupling in DQF-COSY (data not shown). In both variants, residues 8–11, UUCG, form a tetraloop structure as indicated by nonstandard structural constraints in the loop region: presence of G11 in *syn* conformation, U9 and C10 sugars in 2′-*endo* conformation, and strong NOEs between C10 aromatic protons and U8 and U9 sugar protons (7).

Structure of the 3′ Terminus. The two variants adopt different conformations at their 3′ ends.

A19 variant. The 3′ end of the A19 variant maintains a stacked conformation throughout the ACCA sequence. Internucleotide NOEs that are consistent with A-form stacking are observed from C18 through A22 (Fig. 2*A*). In particular, strong H8/H6 to $n - 1$ H2′ NOEs are observed even at NOESY mixing times of 50 ms. NOEs are observed between A19(H2) and both G1(H1′) and C20(H1′); these NOEs are also expected from A-form stacking geometry. No NOEs are observed from A22 (H8). Only A22 and C21 have observable H1′–H2′ cross-peaks in a DQF-COSY experiment, consistent with the presence of C2′-*endo* conformation (data not shown). These data further support the A-form stacking of the 3′ end of the A19 variant.

U19 variant. The 3′ end of the U19 variant does not adopt an extended stacked conformation. The first indication for this comes from DQF-COSY data at 25°C, which show that the riboses of A22–U19 all adopt large fractions of 2′-*endo* conformation (data not shown). Strong H6–($n - 1$)H2′ NOEs are observed between C20 and U19 and U19 and C18. These NOEs are consistent with the stacking of these nucleotides. However, a break in the internucleotide NOE connectivity is observed between C20 and C21. Although spectral overlap at 25°C prevents an unambiguous statement, no C21(H6)–C20(H1′) NOE is observed at either 10°C or 37°C. The C21(H6) to C20(H2′) NOE is very weak. Stacking NOEs are observed between A22 and C21.

Long-range NOEs suggest a distorted and folded-back structure for the 3′ end of the U19 variant. Most importantly, two NOEs are observed between A22 and G1, which indicate

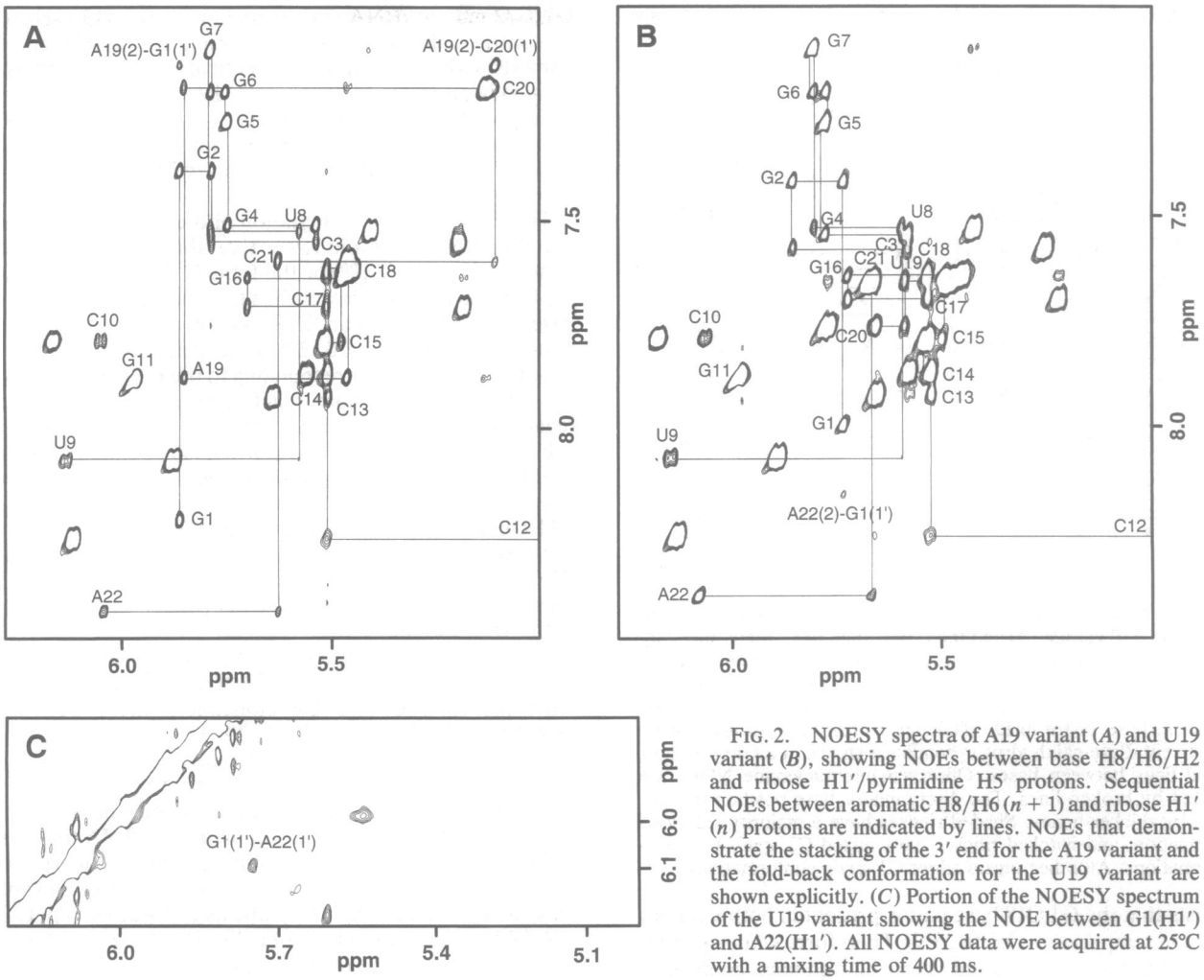

FIG. 2. NOESY spectra of A19 variant (*A*) and U19 variant (*B*), showing NOEs between base H8/H6/H2 and ribose H1′/pyrimidine H5 protons. Sequential NOEs between aromatic H8/H6 ($n + 1$) and ribose H1′ (n) protons are indicated by lines. NOEs that demonstrate the stacking of the 3′ end for the A19 variant and the fold-back conformation for the U19 variant are shown explicitly. (*C*) Portion of the NOESY spectrum of the U19 variant showing the NOE between G1(H1′) and A22(H1′). All NOESY data were acquired at 25°C with a mixing time of 400 ms.

that the 3′ end is folded back such that the 5′- and 3′-terminal nucleotides are in close proximity. The observed NOEs [A22(H2)–G1(H1′) (Fig. 2*B*) and A22(H1′)–G1(H1′) (Fig. 2*C*)] are consistent with stacking of A22 on G1. In addition, nonstandard NOEs are observed from the A22(H2) to C21(H4′) and C20(H2′).

NMR spectra obtained at 10°C, 25°C, and 37°C indicate that the conformations at the 3′ end of both structures are not drastically affected by changes in temperature in this range. The A19 variant adopts the same stacked conformation over this temperature range. For the U19 variant, the long-range NOEs that indicate the fold-back conformation of the 3′ end are observed at all temperatures. However, minor changes in conformation are observed. At 10°C, only A22 and C21 riboses adopt majority 2′-*endo* conformations, whereas at 25°C A22 through U19 riboses adopt 2′-*endo* conformations. Several weak NOEs, A22(H8) to C21(H1′), A22(H2) to C20(H2′), and A22(H2) to C21(H4′), which are present at 10°C and 25°C, are not observed at 37°C.

DISCUSSION

Effect of Discriminator Base on tRNA Structure at the 3′ End. Our results show that the nature of the discriminator base determines the conformation of the 3′ end of the tRNA, assuming that conformations of tRNA acceptor stem microhelices (17) reflect the conformation of the full-length tRNAs (Fig. 3). We characterized the conformation of two RNA oligonucleotides which correspond to the acceptor stem of mutants of $tRNA^{fMet}$ and which differ only in the discriminator base. An A at the discriminator position yields a structure in which the 3′-ACCA sequence continues the A-form stacking of the acceptor stem, as seen in the x-ray structure of yeast $tRNA^{Phe}$ (18, 19). A U at the discriminator position disrupts the continuous stacking of the 3′ end. For the latter oligonucleotide, the NMR data strongly support a conformation in which the 3′ end is folded back such that A22 (corresponding to A76 in tRNA) and G1 are in close proximity. It is possible that a weak base pair is formed between A22 and U19, forming a structure similar to the stable UUCG or GNRA tetraloops (9, 20). The main result is that the identity of the discriminator base affects the structure of the 3′ terminus of the acceptor stem.

The NMR data suggest different populations of the two conformers in the two variants. For the A19 variant, at no temperature do we see any long-range NOEs indicative of the fold-back structure. In contrast, for the U19 variant, the presence of the A22 to G1 NOEs indicates a significant population of the fold-back structure. Although the energy differences may be small, there is a clear difference in the stability of the fold-back conformation relative to the extended conformation in the two variants.

The NMR data show differences in the chemical shift and in the temperature dependence of the G1·C18 imino proton spectra of the two variants (Fig. 1 *B* and *C*). The G1·C18 imino proton resonance of the U19 variant broadens at lower temperature (37°C) than that of the A19 variant. This indicates a difference in the kinetics of imino proton exchange for the two variants (21). However, the stability of the terminal G1·C18 base pair cannot be determined from the exchangeable proton kinetic behavior. The NMR evidence, including NOE data from exchangeable and nonexchangeable protons,

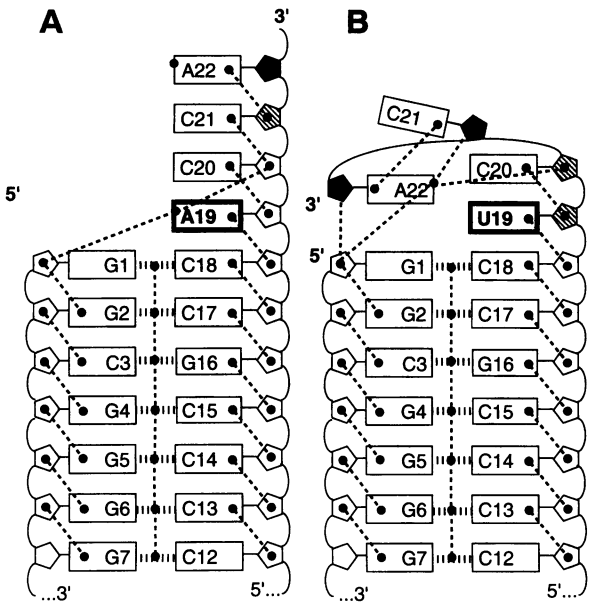

FIG. 3. Schematic representation that summarizes the conformations of the A19 variant (*A*) and the U19 variant (*B*) as determined by NMR spectroscopy at 25°C. Bases are indicated by rectangles and ribose sugars by pentagons. Ribose, base H8/H6, adenine H2, and imino protons are represented by dots within pentagons, on the outside of a base, on the inside of adenines, or within hydrogen bonds, respectively. Base-pair hydrogen bonding is shown by a series of short vertical lines between bases. Observed internucleotide NOEs are indicated by broken lines. The discriminator base position is highlighted by thicker boxes. Shaded riboses have a majority C2′-*endo* conformation, and hatched riboses have mixed C2′-*endo*–C3′-*endo* conformations. All other sugars adopt C3′-*endo* conformations.

suggests that the G1·C18 base pair is present in both variants at least at temperatures up to 25°C. Therefore, while opening of the G1·C18 base pair could favor the fold-back conformation seen with the U19 variant (see below), it is not essential for its formation.

X-ray crystallographic studies indicate that $tRNA^{fMet}$ also has a fold-back conformation, which may be "similar" to that of the U19 variant, although the position of the 3′-terminal A76 is not fixed in the crystal structure (22). In addition, results of electron paramagnetic resonance studies on spin-labeled $tRNA^{fMet}$ (23), studies of the RNA ligase-catalyzed intramolecular joining of 3′-OH of $tRNA^{fMet}$ to the 5′-phosphate leading to its circularization (24), and fluorescence energy transfer studies (25) are in general consistent with a fold-back structure for the tRNA. The acceptor stem of $tRNA^{fMet}$ differs from the A19 variant only in that the former has a C1×A72 mismatch (26), whereas the latter has a G·C base pair at the corresponding position. Thus, the C1×A72 mismatch in $tRNA^{fMet}$ favors the formation of a fold-back structure even when the discriminator base is A. Therefore, either lack of a 1·72 base pair or presence of U73 favors the fold-back conformation for tRNA.

Correlation Between Structure of Oligonucleotides and Function of tRNA. Propensities to form distinct structures can be used by proteins to distinguish among tRNAs (27), and different proteins may use different structural features for discrimination. As noted above, the fold-back structure observed for the U19 variant may be "similar" to that observed for $tRNA^{fMet}$. Therefore, the fold-back structure could have a role in tRNA function. If so, it is more likely to be in recognition of $tRNA^{fMet}$ by Met-tRNA transformylase than by methionyl-tRNA synthetase (MetRS). The G1·C72/U73 mutant tRNA corresponding to the U19 variant is ≈16-fold better as substrate for Met-tRNA transformylase than the G1/C72 mutant tRNA corresponding to the A19 variant (6). In contrast, the tRNAs corresponding to the A19 and U19 variants exhibit essentially identical V_{max}/K_m values for aminoacylation by MetRS (C. P. Lee and U.L.R., unpublished observations; see also ref. 4). Thus, the Met-tRNA transformylase may discriminate among substrates on the basis of the fold-back conformation, while MetRS probably does not.

The V_{max}/K_m^{app} for formylation of the G1·C72/U73 mutant initiator tRNA is 60-fold lower than that of $tRNA^{fMet}$ (6). In contrast the V_{max}/K_m^{app} for the C1·G72/U73 mutant initiator tRNA is only 3.7-fold lower than that for $tRNA^{fMet}$ (4). A C·G base pair at the end of an RNA helix is considered less stable than a G·C base pair (28, 29). In addition, the C in the C·G base pair in a tRNA corresponding to the U19 variant, but not the A19 variant, is more reactive to single-strand-specific reagents such as sodium bisulfite (6). Therefore, the best substrate for Met-tRNA transformylase could be a tRNA in which the 1·72 base pair is broken and the A76 is folded back towards the acceptor stem. It will be interesting to perform NMR analyses on sets of oligonucleotides, similar to the A19 and U19 variants, which have C1·G18 base pair instead of the G1·C18 base pair to see (*i*) whether a C1·G18 base pair is present and (*ii*) whether the UCCA sequence is folded back in the U19 variant.

The fold-back conformation could also contribute to discrimination of the initiator tRNA from elongator tRNAs by other proteins such as the elongation factor EF-Tu and peptidyl-tRNA hydrolase (4, 6, 30–33). These proteins and Met-tRNA transformylase all interact with tRNAs that have either an amino acid or a peptide moiety attached to the 3′ end of tRNA. It is, therefore, important to determine whether the fold-back conformation is maintained in an RNA that has an amino acid or peptide attached to the 3′ end. It is also possible that the fold-back conformation has a role in protein synthesis at a step subsequent to synthesis of fMet-tRNA (1, 2).

A fold-back conformation of a different type was observed in the crystal structure of the complex of *E. coli* $tRNA^{Gln}$ with glutaminyl-tRNA synthetase (GlnRS) (34). In this structure, the U1·A72 base pair of $tRNA^{Gln}$ is broken and the 3′ end folds back to the minor groove side of the acceptor stem, making a hairpin turn such that A76 is closer to C71. This structure is stabilized by G73's forming a specific hydrogen bond with phosphate 72. While the structure of $tRNA^{Gln}$ is not known, the fold-back conformation of $tRNA^{Gln}$ is probably formed only upon binding to GlnRS. In contrast to the fold-back conformation of $tRNA^{Gln}$ in the $tRNA^{Gln}$-GlnRS complex, the U19 variant that we have studied forms a structure in which the 3′ end folds back towards the major groove side of the acceptor stem such that A76 in the corresponding tRNA would be closer to G1. These differences in conformation between the 3′ ends of *E. coli* $tRNA^{Gln}$ in the $tRNA^{Gln}$-GlnRS complex and the U19 variant and the role of G73 in stabilizing the $tRNA^{Gln}$ conformation could explain the opposite effects of A73 → G73 mutation on recognition of *E. coli* initiator tRNA by Met-tRNA transformylase and by GlnRS (4, 35).

If the presence of U in the discriminator position leads to a fold-back structure of the type we have observed, this raises the question of whether such a structure contributes in any way towards aminoacylation of tRNAs that contain U73. This will depend in part upon how close the fold-back and the extended conformations are energetically to the conformation of tRNA required for aminoacylation. Cysteine and glycine tRNAs of *E. coli* and glutamine tRNAs of eukaryotic cytoplasm contain U73 (36). The first four base pairs in the acceptor stem of *E. coli* $tRNA^{Cys}$ are, in fact, identical to those of the U19 variant studied here. Therefore, *E. coli* $tRNA^{Cys}$ could have a fold-back structure at the 3′ end. Mutations of U73 in *E. coli* $tRNA^{Cys}$ to any of the other three

nucleotides lower V_{max}/K_m^{app} in aminoacylation by factors of 3200 for C73, 13,000 for A73, and >13,000 for G73 (37). Such large effects on aminoacylation suggest that U73 is a site of direct contact for cysteinyl-tRNA synthetase (CysRS). However, part of the effect of these mutations could also be due to a preference of CysRS for tRNA with a fold-back structure. It is interesting that U73 is strictly conserved in $tRNA^{Cys}$ of eubacteria, archaebacteria, and eukaryotic cytoplasm.

In conclusion, the results of NMR analyses of oligonucleotides corresponding to the acceptor stem have further highlighted the role of the discriminator base in influencing tRNA conformation at the 3′ end (6). Many proteins, including aminoacyl-tRNA synthetases and RNA enzymes such as the M1 RNA component of RNase P, utilize the acceptor stem and 3′ end of tRNA for binding discrimination (3, 4, 6, 30, 33, 34, 38–44). Therefore, it is important to consider in all of these cases the contribution of 3′-terminal conformation on specific recognition of tRNAs.

We thank C. Ming Chow for her help during this work, C. Ming Chow, Sidney Altman, and Richard Giege for comments and valuable suggestions on the manuscript, and Annmarie McInnis for her usual care and cheerfulness in the preparation of this manuscript. This work was supported by Grant GM17151 from the National Institutes of Health to U.L.R. and by a grant from the Searle Scholars Program of the Chicago Community Trust to J.R.W. The NMR facility at the University of California at Santa Cruz was supported by a grant from the Markey Foundation to the Center for the Molecular Biology of RNA.

1. Kozak, M. (1983) *Microbiol. Rev.* **47**, 1–45.
2. RajBhandary, U. L. (1994) *J. Bacteriol.* **176**, 547–552.
3. Lee, C. P., Seong, B. L. & RajBhandary, U. L. (1991) *J. Biol. Chem.* **266**, 18012–18017.
4. Lee, C. P., Dyson, M. R., Mandal, N., Varshney, U., Bahramian, M. B. & RajBhandary, U. L. (1992) *Proc. Natl. Acad. Sci. USA* **89**, 9262–9266.
5. Guillon, J.-M., Meinnel, T., Mechulam, Y., Lazennec, C., Blanquet, S. & Fayat, G. (1992) *J. Mol. Biol.* **224**, 359–367.
6. Lee, C. P., Mandal, N., Dyson, M. R. & RajBhandary, U. L. (1993) *Proc. Natl. Acad. Sci. USA* **90**, 7149–7152.
7. Varani, G. & Tinoco, I., Jr. (1991) *Quart. Rev. Biophys.* **24**, 479–532.
8. Crothers, D. M., Seno, T. & Soll, D. (1972) *Proc. Natl. Acad. Sci. USA* **69**, 3063–3067.
9. Varani, G., Cheong, C. & Tinoco, I., Jr. (1991) *Biochemistry* **30**, 3280–3289.
10. Milligan, J. F. & Uhlenbeck, O. C. (1989) *Methods Enzymol.* **180**, 51–62.
11. Wyatt, J. R., Chastain, M. & Tinoco, I., Jr. (1991) *BioTechniques* **11**, 764–769.
12. Silberklang, M., Gillum, A. M. & RajBhandary, U. L. (1979) *Methods Enzymol.* **59**, 58–109.
13. Hore, P. J. (1983) *J. Magn. Reson.* **55**, 283–300.
14. Smallcombe, S. (1993) *J. Am. Chem. Soc.* **115**, 4776–4785.
15. Puglisi, J. D., Tan, R., Calnan, B. J., Frankel, A. D. & Williamson, J. R. (1992) *Science* **257**, 76–80.
16. Puglisi, J. D., Wyatt, J. R. & Tinoco, I., Jr. (1990) *J. Mol. Biol.* **214**, 437–453.
17. Francklyn, C. & Schimmel, P. (1989) *Nature (London)* **337**, 478–481.
18. Kim, S. H., Suddath, F. L., Quigley, G. J., McPherson, A., Sussman, J. L., Wang, A. H. J., Seeman, N. C. & Rich, A. (1974) *Science* **185**, 435–440.
19. Robertus, J. D., Ladner, J. E., Rhodes, D., Brown, R. S., Clark, B. F. C. & Klug, A. (1974) *Nature (London)* **250**, 546–551.
20. Heus, H. A. & Pardi, A. (1991) *Science* **253**, 191–194.
21. Limmer, S., Hoffmann, H.-P., Ott, G. & Sprinzl, M. (1993) *Proc. Natl. Acad. Sci. USA* **90**, 6199–6202.
22. Woo, N. H., Roe, B. A. & Rich, A. (1980) *Nature (London)* **286**, 346–351.
23. Pscheidt, R. H. & Wells, B. D. (1986) *J. Biol. Chem.* **261**, 7253–7256.
24. Bruce, A. G. & Uhlenbeck, O. C. (1978) *Nucleic Acids Res.* **5**, 3665–3677.
25. Ferguson, B. Q. & Yang, D. C. H. (1986) *Biochemistry* **25**, 6572–6578.
26. Dube, S. K., Marcker, K. A., Clark, B. F. C. & Cory, S. (1968) *Nature (London)* **218**, 232–233.
27. Steitz, T. A. (1990) *Quart. Rev. Biophys.* **23**, 205–280.
28. Sugimoto, N., Kerzek, R. & Turner, D. H. (1987) *Biochemistry* **26**, 4554–4558.
29. Turner, D. H., Sugimoto, N. & Freier, S. M. (1988) *Annu. Rev. Biophys. Biophys. Chem.* **17**, 167–192.
30. Seong, B. L. & RajBhandary, U. L. (1987) *Proc. Natl. Acad. Sci. USA* **84**, 8859–8863.
31. Kossel, H. & RajBhandary, U. L. (1968) *J. Mol. Biol.* **35**, 539–560.
32. Schulman, L. H. & Pelka, H. (1975) *J. Biol. Chem.* **250**, 542–547.
33. Dutka, S., Meinnel, T., Lazennec, C., Mechulam, Y. & Blanquet, S. (1993) *Nucleic Acids Res.* **21**, 4025–4030.
34. Rould, M. A., Perona, J. J., Soll, D. & Steitz, T. A. (1989) *Science* **246**, 1135–1142.
35. Dyson, M. R., Mandal, N. & RajBhandary, U. L. (1993) *Biochimie* **75**, 1051–1060.
36. Sprinzl, M., Hartman, T., Weber, J., Blank, J. & Zeidler, R. (1989) *Nucleic Acids Res.* **17**, r1–r172.
37. Komatsoulis, G. A. & Abelson, J. (1993) *Biochemistry* **32**, 7435–7444.
38. Moras, D. (1992) *Trends Biochem. Sci.* **17**, 159–164.
39. Schimmel, P., Giege, R., Moras, D. & Yokoyama, S. (1993) *Proc. Natl. Acad. Sci. USA* **90**, 8763–8768.
40. McClain, W. H. (1993) *FASEB J.* **7**, 72–78.
41. Shimizu, M., Asahara, H., Tamura, K., Hasegawa, T. & Himeno, H. (1992) *J. Mol. Evol.* **35**, 436–443.
42. Breitschopf, K. & Gross, H. J. (1994) *EMBO J.* **13**, 3166–3169.
43. Perreault, J.-P. & Altman, S. (1992) *J. Mol. Biol.* **226**, 399–409.
44. Kirsebom, L. A. & Svärd, S. G. (1994) *EMBO J.* **13**, in press.